RF shimming using a multi-element transmit system in phantom and in vivo studies

U. Katscher[1], P. Vernickel[1], I. Graesslin[1], and P. Boernert[1]
[1]Philips Research Laboratories, Hamburg, Germany

Introduction: Wave propagation effects diminish the quality of MR images at main fields of 3T or above, in particular in abdominal applications. Parallel RF transmission techniques bear the potential of compensating for these effects through RF shimming. RF shimming can be performed in two different ways. The basic way of RF shimming is to adjust the global amplitude and phase of the currents in each transmit element, aiming for a constant B_1 amplitude in the region of interest [1-3]. On the other hand, "tailored" RF shimming can be performed via spatially selective RF pulses [4], designed to achieve a spatially constant excitation pattern [5]. With parallel transmission, these RF pulses might be shortened to feasible pulse durations [6-8]. This study compares the two approaches experimentally using a whole-body, eight-channel Tx/Rx system at 3T.

Theory: The central equation for both, the basic and tailored RF shimming, is given by

$$R(\mathbf{x})\sum_{n=1}^{N} T_n(\mathbf{x})P_n(\mathbf{x}) = C \quad . \tag{1}$$

Eq. (1) states, that the superposition of the transmit sensitivity profiles $T_n(\mathbf{x})$ of the N transmit coils, weighted with $P_n(\mathbf{x})$, yields the desired constant B_1 distribution C. If non-constant, also the sensitivity $R(\mathbf{x})$ of the receive coil has to be taken into account (for the sake of simplicity, a single receive coil is assumed). For the basic RF shimming, $P_n(\mathbf{x})$ are constant, leading to a global (complex) scaling of the different sensitivity profiles $T_n(\mathbf{x})$. This problem can be solved, e.g., by discretizing Eq. (1) on a spatial grid of M pixels and inverting the resulting vector/matrix equation

$$\underline{\underline{S}}\,\underline{P} = \underline{C} \quad . \tag{2}$$

Here, $\underline{P}$ is a vector containing the N complex weighting factors P_n for the transmit elements, and $\underline{C}$ is a vector with M constant complex components reflecting the grey values of the constant target pattern discretized on the spatial grid. The $N\times M$ matrix $\underline{\underline{S}}$ contains the spatially discretized sensitivities

$$S_{nm} = R(\mathbf{x}_m)T_n(\mathbf{x}_m) \quad . \tag{3}$$

However, in the majority of applications, only a constant amplitude $|C|$ is required, and an arbitrary spatial phase distribution is acceptable. This is the case, if only magnitude images are of interest. The resulting degree of freedom enhances the power of basic RF shimming considerably, however, it makes Eq. (1) non-linear. In this study, a simulated annealing approach [9] is used to optimize the function globally in combination with a multidimensional Powell method [9] to optimize the solution of the previous step locally.

For the tailored RF shimming, $P_n(\mathbf{x})$ of Eq. (1) define spatial excitation patterns of the individual transmit elements, which can be converted to (multi-dimensional) RF pulses [4]. The simultaneous use of multiple transmit elements allows the shortening of the different pulses [6,7], e.g., via solving

$$\underline{\underline{s}}_{full}(\mathbf{k}-\mathbf{k}_{red})\,\underline{p}_{full}(\mathbf{k}_{red}) = \underline{c}(\mathbf{k}) = \underline{\delta}(\mathbf{k}-\mathbf{k}_0) \quad . \tag{4}$$

The vector $\underline{p}_{full}$ contains the spatially selective RF pulses of the different transmit elements. The vector $\underline{c}$ is the discretized constant target pattern, i.e., a delta function in k-space. The matrix $\underline{\underline{s}}_{full}$ is calculated from the transmit and receive sensitivities [6].

Methods: A 3T MR system (Philips Achieva, Philips Medical System, Best, The Netherlands) was equipped with an 8-element body coil and the corresponding RF channels capable for parallel transmission [10,11]. The sensitivity products $R(\mathbf{x})T_n(\mathbf{x})$ as required by Eq. (1) were approximated by a single low flip angle image per transmit coil (3D FFE, TR/TE=5/2.4ms, resolution 8×8×30mm, α=3°) to save acquisition time. For signal reception, the eight elements of the body coil were combined to a single receive coil. For the phantoms, the sensitivities were also simulated using a model of the 8-element body coil in the Method-of-Moments tool FEKO (EMSS, Stellenbosch, South Africa). Spatially selective RF pulses with reduction factors ρ=1/2 were applied, i.e., spiral trajectories with 8/16 revolutions for a field of excitation of 32² pixels. In the imaging experiments, the same sequence was used as for the sensitivity determination, however, with higher spatial resolution (1.7×1.7×20mm).

Results/Discussion: The potential of basic RF shimming depends significantly on the geometry of the investigated object. The simulations show, that small phantoms in the isocenter can be shimmed to a high degree, at least in the regarded central slice [1]. With increasing diameter and off-center, the quality of the shimming decreases, especially for spherical objects (Fig. 1a/b). At least in the investigated scenario, basic RF shimming works better for B_0 = 3T than for B_0 = 7T (Fig. 1c). Experimentally, it turned out, that transverse images of the human abdomen can be shimmed to an acceptable level with basic RF shimming (Fig. 2). For large spherical objects, tailored RF shimming via (shortened) spatially selective RF pulses is superior compared with basic RF shimming (Table 1).

Conclusion: Basic RF shimming via the adjustment of amplitude and phase of each transmit element seems to be sufficient for the majority of applications. The remaining inhomogeneities of a few percent may be disturbing while imaging homogeneous phantoms. However, in patient images, the remaining inhomogeneities are less apparent due to the inhomogeneous patient morphology, and thus, negligible.

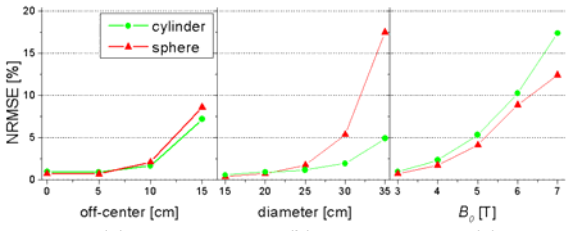

Fig. 1: Simulated normalized root-mean-square error (NRMSE) for basic RF shimming in an eight-element body coil. (a) NRMSE vs. off-center for two objects (Ø = 20 cm). (b) NRMSE vs. diameter for two isocenter objects. (c) NRMSE vs. B_0 for two isocenter objects (Ø = 20 cm).

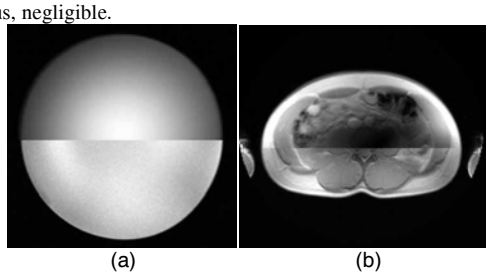

Fig. 2: Experimental results with (lower half) and without (upper half) basic RF shimming. (a) Cylindrical phantom, doped water (∅ = 16 cm). (b) Abdominal example.

Method	NRMSE
basic RF shimming, constant phase	0.85
basic RF shimming, arbitrary phase	0.34
tailored RF shimming, reduction factor ρ = 1	0.24
tailored RF shimming, reduction factor ρ = 2	0.27

Table 1: List of different experimental NRMSE for a large spherical phantom (∅ = 27.5 cm), scaled to the result without shimming.

References: [1] Hoult DI et al., JMRI 12 (2000) 46 [2] Ibrahim TS et al., MRI 18 (2000) 733 [3] Seifert F et al., ISMRM 10 (2002) 162 [4] Pauly J JMR 81 (1989) 43 [5] Saekho S et al., MRM 53 (2005) 479 [6] Katscher U et al., MRM 49 (2003) 144 [7] Zhu Y, MRM 51 (2004) 775 [8] Ullmann P et al., MRM 54 (2005) 994 [9] Press W et al., *Numerical recipes in C,* Cambridge University Press; 1992 [10] Graesslin I et al., ISMRM 14 (2006) 129 [11] Vernickel P et al., ISMRM 14 (2006) 123